

1 ***Gene expression genetics of the striatum of Diversity Outbred mice***

2

3 **Authors**

4 Vivek M. Philip¹, Hao He², Michael C. Saul¹, Price E. Dickson³, Jason A. Bubier¹,

5 Elissa J. Chesler¹

6

7 **Affiliations**

8 1. The Jackson Laboratory for Mammalian Genetics, Bar Harbor, ME 04605

9 2. The Jackson Laboratory for Genomic Medicine, Farmington, CT 06032

10 3. Department of Biomedical Sciences, Joan C. Edwards School of Medicine

11 Marshall University, 1700 3rd Ave. Huntington, WV 25703

12

13

14 corresponding author(s):

15 Elissa J. Chesler (Elissa.Chesler@jax.org)

16 The Jackson Laboratory

17 600 Main Street

18 Bar Harbor ME 04609

19

1 **Abstract**

2

3 Brain transcriptional variation is a heritable trait that mediates complex behaviors,
4 including addiction. Expression quantitative trait locus (eQTL) mapping reveals
5 genomic regions harboring genetic variants that influence transcript abundance. In this
6 study, we profiled transcript abundance in the striatum of 386 Diversity Outbred
7 (J:DO) mice of both sexes using RNA-Seq. All mice were characterized using a
8 behavioral battery of widely-used exploratory and risk-taking assays prior to
9 transcriptional profiling. We performed eQTL mapping, incorporated the results into a
10 browser-based eQTL viewer, and deposited co-expression network members in
11 GeneWeaver. The eQTL viewer allows researchers to query specific genes to obtain
12 allelic effect plots, analyze SNP associations, assess gene expression correlations, and
13 apply mediation analysis to evaluate whether the regulatory variant is acting through
14 the expression of another gene. GeneWeaver allows multi-species comparison of gene
15 sets using statistical and combinatorial tools. This data resource allows users to find
16 genetic variants that regulate differentially expressed transcripts and place them in the
17 context of other studies of striatal gene expression and function in addiction-related
18 behavior.

19

20

21

1 **Background & Summary**

2

3 Substance use disorder is a highly heritable trait involving variation in neural
4 circuitry underlying motivated behavior and behavioral inhibition. Characterization of
5 addiction-related brain regions in genetically diverse mice can lead to the discovery of
6 molecular mechanisms of addiction-related behaviors. These mechanisms can in turn,
7 aid in connecting genetic, genomic and behavioral variation within and across species
8 through shared target genes¹.

9 Drug-induced transcriptional changes in the corticostriatal system have been
10 reported in rodent models^{2,3} and substance dependent individuals^{4,5}. Additionally,
11 behavioral correlates of substance use disorder, namely impulsivity and incentive
12 sensitization, all involve corticostriatal circuitry⁶⁻¹⁰; however, the molecular
13 mechanisms underlying these relationships are unknown. The striatum plays a central
14 role in addiction-related behavior^{11,12} and influences behaviors (e.g., sensation
15 seeking) that predict the development of substance use disorders¹³⁻¹⁶. It receives
16 inputs from diverse brain regions, including the midbrain, prefrontal cortex, and
17 thalamus, and plays a fundamental role in goal-directed actions and habits¹¹. The
18 dopamine projections from the ventral tegmental area to the nucleus accumbens and
19 prefrontal cortex are at the heart of this reward circuit, and their importance to drug
20 reward is well established¹⁷. Neuroimaging studies of people with a history of cocaine
21 use disorders and rodent studies have indicated that addiction is a circuit-level
22 disorder involving several functionally inter-connected brain regions^{18,19}. Identifying
23 drug-induced changes in gene expression^{20,21} and resulting neural plasticity^{22,23} in
24 addiction-relevant neurocircuits can reveal underlying sources of addiction risk and
25 resilience.

1 Gene expression quantitative trait locus (eQTL) and systems genetic analyses
2 facilitate the identification of genes and variants associated with complex traits,
3 including those related to addiction.²⁴ Such data allow the reduction of large numbers
4 of positional candidate genes and variants implicated in quantitative trait locus (QTL)
5 for behavioral traits. These data are also useful for discovering transcripts significantly
6 correlated with behavior and uncovering transcriptional co-expression networks to
7 identify the biomolecular mechanisms underlying complex traits²⁴. Researchers can
8 also use eQTL data to identify genetic variants regulating differentially expressed
9 genes, such as those discovered in drug exposure studies. This data can be used with
10 data from other model organisms²⁵ to identify convergent evidence for biological
11 mechanisms of addiction across species^{26,27}. Model organism eQTLs can also be
12 related to convergent findings in humans to prioritize genome-wide association study
13 (GWAS) results and to contextualize the role of the identified variant¹.

14 To ensure variation in nearly every gene in the genome and to increase the
15 precision of QTL mapping, the Diversity Outbred²⁸⁻³⁰ (J:DO) mice were developed as
16 an advanced intercross of the eight-way hybrid Collaborative Cross (CC)
17 population^{31,32}. Within the J:DO population, there are over 45 million single-
18 nucleotide polymorphisms (SNPs) and millions of insertions and deletions
19 segregating^{12,33,34}. This high genetic diversity results in high phenotypic and
20 transcriptomic variation^{35,36}, enabling the discovery of genes and variants associated
21 with behaviors.

22 Transcription regulatory variation is often context specific. Studies of
23 transcriptional variation in J:DO mice have revealed precise genetic variation

1 affecting proteomes and cellular transcriptional states in addition to bulk
2 transcriptomics of tissues relevant to metabolism in health and disease³⁷⁻³⁹.

3 To construct a versatile reference data resource for addiction genetics, we
4 performed a series of addiction-relevant exploratory and risk-taking behavioral
5 assays^{35,40}, and then profiled transcript abundance in striatum using RNA-Seq on 368
6 drug naïve J:DO mice. Data from this study are delivered in a platform that allows for
7 the identification of eQTL effects, analysis of local SNP associations, assessment of
8 gene expression correlations, and application of mediation analysis. This provides a
9 resource for genetic studies of transcriptional diversity in the striatum of drug naïve
10 mice. Combined with behavioral phenotyping, this resource enables the prioritization
11 of behavioral QTL positional candidates by incorporating evidence from strong cis-
12 eQTL effects and their underlying allelic patterns. Furthermore, behavioral QTLs can
13 be subjected to local SNP association analysis followed by prioritization of positional
14 candidates where the SNP strain distribution pattern of positional candidates matches
15 the allelic effects of interest. Positional candidates can then be queried in this resource
16 for the presence or absence of strong cis-eQTLs. Finally, the data can be used in
17 global analyses of the relationship of trait-relevant variation across species, using
18 increasingly sophisticated approaches for leveraging model organism data to predict,
19 model, and explain polygenic risk for human disease⁴¹⁻⁴³.

20

1 **Methods**

2 **Mice**

3 416 J:DO mice (strain #:009376) from both sexes, spanning generations G21, G22,
4 and G23, were purchased from The Jackson Laboratory. The mice were housed in an
5 elevated barrier pathogen- and opportunistic-free animal room (Health report available
6 at: [https://www.jax.org/-/media/jaxweb/health-](https://www.jax.org/-/media/jaxweb/health-reports/g200.pdf?la=en&hash=7AD522E82FA7C6D614A11EFB82547476157F00E1)
7 [reports/g200.pdf?la=en&hash=7AD522E82FA7C6D614A11EFB82547476157F00E1](https://www.jax.org/-/media/jaxweb/health-reports/g200.pdf?la=en&hash=7AD522E82FA7C6D614A11EFB82547476157F00E1)
8) before being transferred at weaning to an intermediate barrier specific pathogen-free
9 room ([https://www.jax.org/-/media/jaxweb/health-](https://www.jax.org/-/media/jaxweb/health-reports/g3b.pdf?la=en&hash=914216EE4F44ADC1585F1EF219CC7F631F881773)
10 [reports/g3b.pdf?la=en&hash=914216EE4F44ADC1585F1EF219CC7F631F881773](https://www.jax.org/-/media/jaxweb/health-reports/g3b.pdf?la=en&hash=914216EE4F44ADC1585F1EF219CC7F631F881773)).
11 Mice were individually housed under (12:12) light/dark cycle and allowed *ad libitum*
12 access to standard rodent chow [sterilized NIH31 5K52 6% fat chow (LabDiet/PMI
13 Nutrition, St. Louis, MO)] and acidified water (pH 2.5–3.0) supplemented with
14 vitamin K. Mice cages contained a pine-shaving bedding (Hancock Lumber) and
15 environmental enrichment consisting of a nestlet and a Shepard’s Shack. The mice
16 were identified by ear notching at weaning and moved between cages and testing
17 using metal forceps.

18 **Behavioral Phenotyping**

19 At three to six months of age, mice were phenotyped four separate times with a
20 different assay on each day, Monday to Thursday (open field, light-dark, hole-board,
21 and novelty place preference)⁴⁴ and euthanized on Friday in batches of 16-24 by
22 decapitation. Phenotyping protocols are available at [https://www.addiction-](https://www.addiction-neurogenetics.org/data-and-resources/)
23 [neurogenetics.org/data-and-resources/](https://www.addiction-neurogenetics.org/data-and-resources/). The Jackson Laboratory (JAX) follows
24 husbandry practices in accordance with the American Association for the

1 Accreditation of Laboratory Animal Care (AAALAC), and all work was done with the
2 approval of the JAX Institutional Animal Care and Use Committee (Approval
3 #10007).

4 **Dissections**

5 Testing and euthanasia were consistently performed between 8 AM to 12 PM to
6 control for circadian effects. All surgical instruments were cleaned with RNAase
7 Away (ThermoFischer Scientific, Waltham, MA) prior to use and between samples.
8 Whole intact brains were removed, hemisected, and incubated in RNAlater
9 (ThermoFischer Scientific, Waltham, MA) for 8-14 minutes. Then, under a dissection
10 microscope, the striatum, hippocampus, and prefrontal cortex were removed and
11 soaked for 24 hours in RNAlater at room temperature before being stored at -80°C
12 until processing.

13 **RNA Isolation and Sequencing**

14 The striatum was homogenized, and total RNA was isolated using a TRIzol Plus kit
15 (Life Technologies, City, State) with on-the-column DNase digestion according to the
16 manufacturer's instructions. The quality of the isolated RNA was assessed using an
17 RNA 6000 Nano LabChip using an Agilent 2100 Bioanalyzer instrument
18 [RRID:SCR_019389 (Agilent Technologies, Santa Clara, CA)] and a NanoDrop
19 spectrophotometer [RRID:SCR_018042 (ThermoFisher Scientific, Wilmington, DE)].
20 The External RNA Controls Consortium spike-in (ERCC, Ambion, Austin, TX) was
21 added to the samples to allow for normalization in accordance with the core facility's
22 standard operating procedure but was not used in our downstream analyses. An RNA-
23 Seq library was prepared using the KAPA Stranded RNA-Seq Kit with RiboErase
24 (Kappa Biosystems, City, State). Libraries were then pooled and sequenced at The

1 Jackson Laboratory using a 100 bp paired-end process on a HiSeq 2500 (Illumina)
2 sequencing system (RRID:SCR_016383) targeting 40 million read pairs per sample.
3 Sequencing achieved a median read depth of 65.7 million read pairs per sample
4 (range: 31.4 million to 117.4 million reads).

5 **Sequencing Analysis**

6 Raw read data were demultiplexed and converted to FASTQ files. Paired-end FASTQ
7 files from multiple lanes were concatenated together prior to alignment. All paired-
8 end FASTQ files were aligned to the *Mus musculus* GRCm38 reference (GenBank
9 accession number: GCA_000001635.2) with Ensembl v94 (October 2018) annotation
10 using STAR (v2.6.1c) (RRID:SCR_004463) set to produce both genome and
11 transcriptome Binary Alignment Map (BAM) files. STAR was used with default
12 options ensuring that these defaults allowed for a maximum of 10 multi-mapped reads
13 and a maximum of 10 mismatches. Reads exceeding these criteria were excluded from
14 further downstream processing. Expression estimation was performed using the
15 RSEM package (v1.3.0) (RRID:SCR_013027) with --estimate-rspd using the
16 transcriptome BAM files obtained following alignments from STAR. RSEM expected
17 counts per transcript were used for downstream analysis.

18 Expression estimate data were imported into R v3.5.1 (RRID:SCR_001905) using
19 tximport v 1.10.1 (RRID:SCR_016752). Data were TMM-normalized with edgeR
20 v3.24.3 (RRID:SCR_012802) and log-transformed to stabilize variance using
21 voom+limma in limma v3.38.3 (RRID:SCR_010943). We used the biomaRt R
22 package v2.38.0 (RRID:SCR_019214) to annotate the data using the v94 Ensembl
23 archive (oct2018.archive.ensembl.org). Using X and Y chromosome gene expression,
24 we discovered that some samples had sex chromosome aneuploidies (X0 females and

1 partial XXY males), a previously documented phenomenon among J:DO mice⁴⁵.
2 These samples were excluded from downstream analyses. Additionally, we discovered
3 that some samples included choroid plexus contamination. We remediated this
4 contamination by taking the residuals of expression regressed on the log-mean
5 expression of the genes *klotho* (*Kl*, ENSMUSG00000058488) and transthyretin (*Ttr*,
6 ENSMUSG00000061808), which are unambiguous markers for the choroid plexus⁴⁶.

7 **Genotyping, Haplotype Reconstruction and Sample QC**

8 Genotyping was performed on tail biopsies by Neogene Genomics (Lincoln, NE)
9 using the Mouse Universal Genotyping Array (GigaMUGA)⁴⁷ consisting of 143,259
10 markers. Based on published genotype QC workflows⁴⁸, 110,524 markers and 386
11 mice were retained for further analysis.⁴⁸ Genotypes were converted to founder
12 strain-haplotype reconstructions using R/qt12⁴⁹(qt12_0.21-1, <http://kbroman.org/qt12>)
13 (RRID:SCR_018181).

14 **Expression QTL mapping**

15 Prior to eQTL mapping, gene expression counts were obtained by summing expected
16 counts over all transcripts for a given gene. Expression for eQTL analysis was
17 adjusted for choroid plexus contamination by regressing the log-mean of *Kl* and *Ttr* as
18 additive covariates. eQTL mapping was performed on regression residuals of 17,248
19 genes using the R/qt12 package and the founder haplotype regression method. To
20 correct for population structure, kinship matrices were computed with the Leave One
21 Chromosome Out (LOCO) option for kinship correction (<http://kbroman.org/qt12>)⁵⁰.
22 Additive covariates of sex and J:DO generation were used in the eQTL mapping
23 model. Specifically, for each gene, the following linear model was fit,

$$y_i = s_i \beta_s + gen_i \beta_{gen} + \sum_{j=1}^7 g_{ij} \beta_j + \gamma_i + \varepsilon$$

1 where y_i is the gene expression abundance of the i^{th} animal, s_i is the sex of animal
2 i , β_s is the effect of sex, gen_i is the generation of animal i , β_{gen} is the effect of
3 generation, g_{ij} is the founder probability for founder allele j in animal i , β_j is the
4 genotype coefficient, and γ_i is the random effect representing the polygenic influence
5 of animal i as modeled by a kinship matrix. eQTL was categorized as either cis or
6 trans, where cis is defined as eQTLs within +/- 2MB of the transcription start site
7 (TSS) of the gene, and trans are eQTLs further away.

8 **Creation of the eQTL Viewer Object**

9 The results of the eQTL analysis, along with expression estimates, genotypes, and
10 covariates, are encapsulated in an RData object. RData objects are designed for use in
11 R and contain all the objects necessary for reproducing an analysis. We followed the
12 instructions provided by the developers of the eQTL viewer^{51,52}. Specifically, we
13 created the following elements: kinship, map, genotype probabilities (genoprobs),
14 markers, and a dataset object that contains information on the gene annotations,
15 covariates, expression data, and sample annotations.

16 **WGCNA Analysis**

17 RNA-Seq data was analyzed with WGCNA (RRID:SCR_003302)⁵³. A soft
18 thresholding power of 3 was selected using the WGCNA scale-free topology R^2
19 threshold of 0.9 with a signed network with a minimum module size of 30. The

1 correlation calculation utilized was bicor, and modules used numeric labels instead of
2 colors.

3 **Paraclique analysis**

4 RNA-Seq data was analyzed with paraclique⁵⁴ using a bicor with a correlation
5 coefficient threshold of |0.5| (unsigned), minimum seed clique size of 5, minimum
6 finished paraclique size of 10, proportional glom factor of 0.2 for paraclique
7 construction.

8 **Genesets for Analysis in GeneWeaver**

9 Set of genes representing the J:DO striatum eQTL, the WGCNA modules and the
10 paracliques were deposited in GeneWeaver (RRID:SCR_009202)⁵⁵ are accession
11 numbers are found in Supplemental Table 1. In addition the eQTLs have been
12 separated into cis and trans sets and are also presented as sets per chromosome.

13

1 **Data Records**

2

3 **Primary Sequence Data**

4

5 Primary raw paired end RNA-Seq data files (FASTQ formatted) from 416 J:DO mice

6 were submitted to the Sequence Read Archive (SRA) and are available with the GEO

7 ID (GSE162732).

8 **Primary Genotyping Data**

9

10 Raw data has been deposited at the Diversity Outbred Database

11 <https://www.jax.org/research-and-faculty/genetic-diversity-initiative/tools->

12 [data/diversity-outbred-database](https://www.jax.org/research-and-faculty/genetic-diversity-initiative/tools-data/diversity-outbred-database) (RRID:SCR_018180)

13 **Primary Phenotyping Data**

14 Phenotyping data has been deposited at the Mouse Phenome Database

15 (RRID:SCR_003212) under project CSNA03.

16 **QTL Viewer Repository**

17

18 QTL Viewer is an interactive web-based analysis tool allowing users to replicate the

19 analyses reported for a study (**Figure 1**). The tool with the data set described here is

20 available at <https://qtlviewer.jax.org/viewer/CheslerStriatum>. It includes the ability to

21 search various subsets of data from a study, such as phenotypes or expression data,

22 and then visualize data with profile, correlation, LOD, effect, mediation, and SNP

23 association plots (**Figure 2**). Detailed information about the structure of the QTL

24 viewer objects is available at <https://github.com/churchill-lab/qtl->

25 [viewer/blob/master/docs/QTLViewerDataStructures.md](https://github.com/churchill-lab/qtl-viewer/blob/master/docs/QTLViewerDataStructures.md). A complementary dataset

26 from the hippocampus previous described in Skeelly et.al⁵⁶ is already available at

27 <https://churchilllab.jax.org/qtlviewer/DO/hippocampus>

28

29 **QTL Viewer RData object**

1 The primary data record associated with this study is

2 `qtlviewer_DO_Striatum_02102020.Rdata`. This RData object contains the following:

- 3 • `genoprobs` - the genotype probabilities
- 4 • `K` - the kinship matrix created using the leave one chromosome out (loco)
- 5 `method`
- 6 • `map` - list of one element per chromosome, with the genomic position of each
- 7 `marker`
- 8 • `markers` - marker names and positions
- 9 • `dataset.DO_Striatum_416` –
- 10 • `annot.mrna` - annotations of the mRNA data
- 11 • `annot.samples` - sample annotations
- 12 • `covar.info` - specific information about the covariates
- 13 • `covar.matrix` - matrix of covariates data, samples (rows) x covariates
- 14 `(columns)`
- 15 • `data` - expression data, samples (rows) x mRNA (columns). This matrix is
- 16 `used in the eQTL mapping analysis.`
- 17 • `datatype` - type of data set, either mRNA or protein
- 18 • `display.name` - simple display name for the viewer
- 19 • `ensembl.version` - version of Ensembl used to annotate locations
- 20 • `lod.peaks` - LOD peaks over a certain threshold, set to >7 in this dataset

21
22
23
24

1 **Technical Validation**

2 **Blinding and Randomization.** In a population genetics study, mouse genotypes are
3 collected randomly. The J:DO population is bred using a pseudorandom mating
4 scheme, and test mice are obtained from several breeding cohorts. Experimenters are
5 unaware of mouse genotypes and their relationship to gene expression. Coat color
6 diversity in this population may create some experimenter bias in conventional mouse
7 populations, but coat color is rarely a predictor of behavior in J:DO mice. In the ideal
8 genetic population, genotypes are fully randomized, and individuals are all genetically
9 equidistant. Because this is not the case, genetic mapping analyses include a
10 relationship matrix, a structured covariance matrix that estimates the relations among
11 individuals based on genotype similarity. Mice of both sexes are counterbalanced
12 across test runs, with each run containing either male or female mice to avoid
13 pheromonal effects on behavior.

14

15 **RNA quality**

16 RNA quality includes three primary components: integrity, purity, and concentration.
17 RNA integrity was determined by the Agilent Bioanalyzer 2100 using an RNA
18 Integrity Number (RIN). This metric uses the ratio of 28S:18S rRNA to rate RNA
19 quality on a scale of 1-10. The median RIN was 9.1 (range: 7.9-9.9). RNA purity and
20 concentration were determined using a NanoDrop spectrophotometer. Using this
21 method, RNA concentration is determined using absorbance at 260 nm, while purity is
22 determined using the ratio of absorbance at 260 nm to 280 nm (A260:A280) and the
23 ratio of absorbance at 260 nm to 230 nm (A260:A230). The median concentration was
24 74.0 ng/ μ L (range: 9.4-186.3 ng/ μ L), the median A260:A280 ratio was 2.00 (range:

1 1.67-2.06), and the median A260:A230 ratio was 2.02 (range: 0.98-3.23). These
2 values indicated that the RNA quality was sufficient for RNA-Seq analysis.

3 **Heritability of transcript variation**

4 Based on variance accounted for by genotypes across the genome, and an additive
5 covariant of generation, transcript abundance has a median heritability of 0.229, which
6 is about two times the observed median heritability observed initially in the BXD²⁴
7 Cis-eQTLs were highly detectable across the entire genome, as a diagonal band (seen
8 in Figure 1). Trans-eQTLs were independent of each other in the genetically
9 unstructured and large population as would be expected. UNC506203, on chr 1 and
10 40.21 Mbp and is the peak marker for the most number (42) of cis- and trans-eQTL.
11 The largest interval between markers (13.852282 Mbp) that have no eQTL is on the X
12 chromosome. This is all consistent with technically valid eQTL mapping.

13

1 **Usage Notes**

2 There are four means by which the processed drug naïve striatum gene expression
3 datasets can be used. First, users can download the entire processed dataset in the
4 RData format. Once downloaded, it is readily readable in the R programming
5 environment. Second, users can access the data at
6 <https://qtlviewer.jax.org/viewer/CheslerStriatum> and proceed with the eQTL profile
7 by entering their specific gene of interest in the search text box. Thirdly, users can
8 access these data using the QTL viewer API interface ([https://github.com/churchill-](https://github.com/churchill-lab/qtl2api)
9 [lab/qtl2api](https://github.com/churchill-lab/qtl2api)). Finally users can download sets of genes derived from the eQTL data by
10 various methods such as WGCNA and paraclique, from the online data repository and
11 suite of tools GeneWeaver.org.
12

1 **Code Availability**

2 The R scripts and the package versions used for the eQTL analysis and the creation of

3 the QTL viewer RData object are available at

4 <https://github.com/TheJacksonLaboratory/CSNA>

5

6

7

8

1 **Acknowledgments**

2 Major support for this work was from the National Institute on Drug Abuse of the
3 National Institutes of Health (NIH RO1 DA037927; NIH P50 DA 039841, NIH U01
4 DA043809). We thank Tyler Roy and Troy Wilcox for performing the striatum
5 dissections. We thank Gary Churchill and Matthew Vincent for their help with the
6 QTL Viewer. This research was also supported by the Genome and Single Cell
7 Technologies and Computational Sciences Shared Resources of the JAX Cancer
8 Center (P30 CA034196). Finally, we gratefully acknowledge the contribution of Heidi
9 Munger and Genome Technologies at The Jackson Laboratory for expert assistance
10 with this publication.

1 **Author contributions**

2

3 Vivek M. Philip- Wrote the manuscript and performed mapping studies.

4 Hao He – Prepared the genotype probabilities matrix and participated in QTL

5 mapping.

6 Michael C. Saul – Performed the transcriptomic alignments, choroid plexus cleaning,

7 QTL mapping and heritability calculations. Participated in the preparation of the

8 manuscript.

9 Price E. Dickson – Oversaw the behavioral testing of the mice and participated in the

10 preparation of the manuscript.

11 Jason A. Bubier. Coordinated procurement of, scheduling, genotyping, and dissecting

12 of Diversity Outbred mice. Participated in the preparation of the manuscript

13 Elissa J. Chesler. Conceived the project, secured funding, and oversaw the design and

14 execution of the research and the manuscript.

15

1 **Competing interests**

2

3 There are no competing interests to declare from authors of this manuscript.

4

1 **Figure Legends**

2

3 **Figure 1. Screenshot of a query for the gene “*Rab3b*” in QTL Viewer.** QTL results
4 for *Rab3b* expression in the Diversity Outbred (J:DO) mice striatum. Metadata related
5 to the J:DO generation and sex is displayed, and genes co-expressed with the selected
6 gene can be accessed from the correlation tab. The allele effect plots, SNP association
7 mapping, and mediation analysis can also be performed and viewed from the page.

8

9 **Figure 2. The *Rab3b* cis-eQTL data retrieved in QTL Viewer.** **A.** A genome scan
10 for *Rab3b* expression in the Diversity Outbred (J:DO) mice striatum identifies a strong
11 (LOD > 65) cis-eQTL on chromosome 4. **B.** The allele effect plot for the haplotypes
12 of the J:DO that regulate the expression of *Rab3b*. There are strong effects of
13 WSB/EiJ, NZO/HILtJ, and C57BL/6J on the expression in one direction and
14 129S1/SvJ, CAST/EiJ, and A/J in the opposite direction. **C.** SNP association mapping
15 within the QTL peak interval displaying all the SNPs that drive the QTL. Most of the
16 highest score SNPs are around *Rab3b*, as expected for a gene regulated in cis. **D.** The
17 genes that are negatively (*Scp2-ps2*) or positively (*Ttc4*, *0610037L13Rik*, *Zyg11b*)
18 correlated with *Rab3b* expression can be displayed. A scatter plot can be generated for
19 each gene with the gene of interest. **E.** Mediation analysis can be performed on the
20 data set to identify candidate causal mediators. This analysis retests the QTL effect at
21 the locus of interest, iteratively conditioned on candidate mediators. Here the SNP in
22 *Scp2-ps2* creates the greatest LOD drop.

23

24

1 **Supplemental Table 1: Table of J:DO striatum Gene Sets that are in**
2 **GeneWeaver.**
3
4

1 **References**

- 2 1 Reynolds, T. *et al.* Interpretation of psychiatric genome-wide association studies with
3 multispecies heterogeneous functional genomic data integration.
4 *Neuropsychopharmacology* **46**, 86-97 (2021). [https://doi.org/10.1038/s41386-020-](https://doi.org/10.1038/s41386-020-00795-5)
5 [00795-5](https://doi.org/10.1038/s41386-020-00795-5)
- 6 2 Walker, D. M. *et al.* Cocaine Self-administration Alters Transcriptome-wide
7 Responses in the Brain's Reward Circuitry. *Biol Psychiatry* **84**, 867-880 (2018).
8 <https://doi.org/10.1016/j.biopsych.2018.04.009>
- 9 3 Huggett, S. B. *et al.* Genes identified in rodent studies of alcohol intake are enriched
10 for heritability of human substance use. *Alcohol Clin Exp Res* (2021).
11 <https://doi.org/10.1111/acer.14738>
- 12 4 Ribeiro, E. A. *et al.* Gene Network Dysregulation in Dorsolateral Prefrontal Cortex
13 Neurons of Humans with Cocaine Use Disorder. *Sci Rep* **7**, 5412 (2017).
14 <https://doi.org/10.1038/s41598-017-05720-3>
- 15 5 Huggett, S. B. & Stallings, M. C. Genetic Architecture and Molecular Neuropathology
16 of Human Cocaine Addiction. *The Journal of neuroscience : the official journal of the*
17 *Society for Neuroscience* **40**, 5300-5313 (2020).
18 <https://doi.org/10.1523/JNEUROSCI.2879-19.2020>
- 19 6 Jupp, B. & Dalley, J. W. Convergent pharmacological mechanisms in impulsivity and
20 addiction: insights from rodent models. *Br J Pharmacol* **171**, 4729-4766 (2014).
21 <https://doi.org/10.1111/bph.12787>
- 22 7 Jentsch, J. D. & Taylor, J. R. Impulsivity resulting from frontostriatal dysfunction in
23 drug abuse: implications for the control of behavior by reward-related stimuli.
24 *Psychopharmacology (Berl)* **146**, 373-390 (1999).
25 <https://doi.org/10.1007/pl00005483>
- 26 8 Meyer, P. J., King, C. P. & Ferrario, C. R. Motivational Processes Underlying Substance
27 Abuse Disorder. *Curr Top Behav Neurosci* **27**, 473-506 (2016).
28 https://doi.org/10.1007/7854_2015_391
- 29 9 Kalivas, P. W., Pierce, R. C., Cornish, J. & Sorg, B. A. A role for sensitization in craving
30 and relapse in cocaine addiction. *J Psychopharmacol* **12**, 49-53 (1998).
31 <https://doi.org/10.1177/026988119801200107>
- 32 10 Wolf, M. E. The Bermuda Triangle of cocaine-induced neuroadaptations. *Trends*
33 *Neurosci* **33**, 391-398 (2010). <https://doi.org/10.1016/j.tins.2010.06.003>
- 34 11 Everitt, B. J. & Robbins, T. W. Neural systems of reinforcement for drug addiction:
35 from actions to habits to compulsion. *Nature neuroscience* **8**, 1481-1489 (2005).
36 <https://doi.org/10.1038/nn1579>
- 37 12 Belin, D. & Everitt, B. J. Cocaine seeking habits depend upon dopamine-dependent
38 serial connectivity linking the ventral with the dorsal striatum. *Neuron* **57**, 432-441
39 (2008). <https://doi.org/10.1016/j.neuron.2007.12.019>
- 40 13 Lind, N. M. *et al.* Behavioral response to novelty correlates with dopamine receptor
41 availability in striatum of Gottingen minipigs. *Behavioural brain research* **164**, 172-
42 177 (2005). <https://doi.org/10.1016/j.bbr.2005.06.008>
- 43 14 Wittmann, B. C., Daw, N. D., Seymour, B. & Dolan, R. J. Striatal activity underlies
44 novelty-based choice in humans. *Neuron* **58**, 967-973 (2008).
45 <https://doi.org/10.1016/j.neuron.2008.04.027>
- 46 15 Hooks, M. S. *et al.* Individual locomotor response to novelty predicts selective
47 alterations in D1 and D2 receptors and mRNAs. *The Journal of neuroscience : the*
48 *official journal of the Society for Neuroscience* **14**, 6144-6152 (1994).
- 49 16 Gjedde, A., Kumakura, Y., Cumming, P., Linnet, J. & Moller, A. Inverted-U-shaped
50 correlation between dopamine receptor availability in striatum and sensation

- 1 seeking. *Proceedings of the National Academy of Sciences of the United States of*
2 *America* **107**, 3870-3875 (2010). <https://doi.org/10.1073/pnas.0912319107>
- 3 17 Cooper, S., Robison, A. J. & Mazei-Robison, M. S. Reward Circuitry in Addiction.
4 *Neurotherapeutics* **14**, 687-697 (2017). <https://doi.org/10.1007/s13311-017-0525-z>
- 5 18 Nielsen, G. [We are not proud enough]. *Sygeplejersken* **90**, 18-20 (1990).
- 6 19 Luscher, C. The Emergence of a Circuit Model for Addiction. *Annu Rev Neurosci* **39**,
7 257-276 (2016). <https://doi.org/10.1146/annurev-neuro-070815-013920>
- 8 20 James, M. H. Mimicking Human Drug Consumption Patterns in Rat Engages
9 Corticostriatal Circuitry. *Neuroscience* **442**, 311-313 (2020).
10 <https://doi.org/10.1016/j.neuroscience.2020.06.012>
- 11 21 Sadri-Vakili, G. Cocaine triggers epigenetic alterations in the corticostriatal circuit.
12 *Brain Res* **1628**, 50-59 (2015). <https://doi.org/10.1016/j.brainres.2014.09.069>
- 13 22 Bobadilla, A. C. *et al.* Corticostriatal plasticity, neuronal ensembles, and regulation of
14 drug-seeking behavior. *Prog Brain Res* **235**, 93-112 (2017).
15 <https://doi.org/10.1016/bs.pbr.2017.07.013>
- 16 23 Wall, N. R. *et al.* Complementary Genetic Targeting and Monosynaptic Input
17 Mapping Reveal Recruitment and Refinement of Distributed Corticostriatal
18 Ensembles by Cocaine. *Neuron* **104**, 916-930 e915 (2019).
19 <https://doi.org/10.1016/j.neuron.2019.10.032>
- 20 24 Chesler, E. J. *et al.* Complex trait analysis of gene expression uncovers polygenic and
21 pleiotropic networks that modulate nervous system function. *Nat Genet* **37**, 233-242
22 (2005). <https://doi.org/10.1038/ng1518>
- 23 25 Munro, D. *et al.* The regulatory landscape of multiple brain regions in outbred
24 heterogeneous stock rats. *Nucleic Acids Res* **50**, 10882-10895 (2022).
25 <https://doi.org/10.1093/nar/gkac912>
- 26 26 Bubier, J. A. *et al.* Cross-Species Integrative Functional Genomics in GeneWeaver
27 Reveals a Role for Pafah1b1 in Altered Response to Alcohol. *Front Behav Neurosci* **10**,
28 1 (2016). <https://doi.org/10.3389/fnbeh.2016.00001>
- 29 27 Bubier, J. A. *et al.* Identification of a QTL in *Mus musculus* for alcohol preference,
30 withdrawal, and Ap3m2 expression using integrative functional genomics and
31 precision genetics. *Genetics* **197**, 1377-1393 (2014).
32 <https://doi.org/10.1534/genetics.114.166165>
- 33 28 Svenson, K. L. *et al.* High-resolution genetic mapping using the Mouse Diversity
34 outbred population. *Genetics* **190**, 437-447 (2012).
35 <https://doi.org/10.1534/genetics.111.132597>
- 36 190/2/437 [pii]
- 37 29 Chesler, E. J. Out of the bottleneck: the Diversity Outcross and Collaborative Cross
38 mouse populations in behavioral genetics research. *Mamm Genome* **25**, 3-11 (2014).
39 <https://doi.org/10.1007/s00335-013-9492-9>
- 40 30 Churchill, G. A., Gatti, D. M., Munger, S. C. & Svenson, K. L. The Diversity Outbred
41 mouse population. *Mamm Genome* **23**, 713-718 (2012).
42 <https://doi.org/10.1007/s00335-012-9414-2>
- 43 31 Chesler, E. J. *et al.* The Collaborative Cross at Oak Ridge National Laboratory:
44 developing a powerful resource for systems genetics. *Mamm Genome* **19**, 382-389
45 (2008). <https://doi.org/10.1007/s00335-008-9135-8>
- 46 32 Churchill, G. A. *et al.* The Collaborative Cross, a community resource for the genetic
47 analysis of complex traits. *Nat Genet* **36**, 1133-1137 (2004). [https://doi.org/ng1104-](https://doi.org/ng1104-1133)
48 [1133](https://doi.org/ng1104-1133) [pii]
- 49 10.1038/ng1104-1133

- 1 33 Ferraj, A. *et al.* Resolution of structural variation in diverse mouse genomes reveals
2 chromatin remodeling due to transposable elements. *bioRxiv*,
3 2022.2009.2026.509577 (2022). <https://doi.org/10.1101/2022.09.26.509577>
- 4 34 Threadgill, D. W. & Churchill, G. A. Ten years of the Collaborative Cross. *Genetics* **190**,
5 291-294 (2012). <https://doi.org/10.1534/genetics.111.138032>
- 6 35 Logan, R. W. *et al.* High-precision genetic mapping of behavioral traits in the diversity
7 outbred mouse population. *Genes Brain Behav* **12**, 424-437 (2013).
8 <https://doi.org/10.1111/gbb.12029>
- 9 36 Philip, V. M. *et al.* Genetic analysis in the Collaborative Cross breeding population.
10 *Genome Res* **21**, 1223-1238 (2011). <https://doi.org/10.1101/gr.113886.110>
11 gr.113886.110 [pii]
- 12 37 Chick, J. M. *et al.* Defining the consequences of genetic variation on a proteome-
13 wide scale. *Nature* **534**, 500-505 (2016). <https://doi.org/10.1038/nature18270>
- 14 38 Skelly, D. A. *et al.* Mapping the Effects of Genetic Variation on Chromatin State and
15 Gene Expression Reveals Loci That Control Ground State Pluripotency. *Cell Stem Cell*
16 **27**, 459-469 e458 (2020). <https://doi.org/10.1016/j.stem.2020.07.005>
- 17 39 Keele, G. R. *et al.* Regulation of protein abundance in genetically diverse mouse
18 populations. *Cell Genom* **1** (2021). <https://doi.org/10.1016/j.xgen.2021.100003>
- 19 40 Recla, J. M. *et al.* Precise genetic mapping and integrative bioinformatics in Diversity
20 Outbred mice reveals Hydin as a novel pain gene. *Mamm Genome* (2014).
21 <https://doi.org/10.1007/s00335-014-9508-0>
- 22 41 Palmer, R. H. C. *et al.* Multi-omic and multi-species meta-analyses of nicotine
23 consumption. *Transl Psychiatry* **11**, 98 (2021). <https://doi.org/10.1038/s41398-021-01231-y>
- 24 42 Huggett, S. B., Bubier, J. A., Chesler, E. J. & Palmer, R. H. C. Do gene expression
25 findings from mouse models of cocaine use recapitulate human cocaine use disorder
26 in reward circuitry? *Genes Brain Behav* **20**, e12689 (2021).
27 <https://doi.org/10.1111/gbb.12689>
- 28 43 Palmer, R. H. C. *et al.* Integration of evidence across human and model organism
29 studies: A meeting report. *Genes Brain Behav*, e12738 (2021).
30 <https://doi.org/10.1111/gbb.12738>
- 31 44 Binh Tran, T. D. *et al.* Microbial glutamate metabolism predicts intravenous cocaine
32 self-administration in diversity outbred mice. *Neuropharmacology* **226**, 109409
33 (2023). <https://doi.org/10.1016/j.neuropharm.2022.109409>
- 34 45 Chesler, E. J. *et al.* Diversity Outbred Mice at 21: Maintaining Allelic Variation in the
35 Face of Selection. *G3 (Bethesda)* **6**, 3893-3902 (2016).
36 <https://doi.org/10.1534/g3.116.035527>
- 37 46 Sathyanesan, M. *et al.* A molecular characterization of the choroid plexus and stress-
38 induced gene regulation. *Transl Psychiatry* **2**, e139 (2012).
39 <https://doi.org/10.1038/tp.2012.64>
- 40 47 Morgan, A. P. *et al.* The Mouse Universal Genotyping Array: From Substrains to
41 Subspecies. *G3 (Bethesda)* **6**, 263-279 (2015). <https://doi.org/10.1534/g3.115.022087>
- 42 48 Broman, K. W., Gatti, D. M., Svenson, K. L., Sen, S. & Churchill, G. A. Cleaning
43 Genotype Data from Diversity Outbred Mice. *G3 (Bethesda)* **9**, 1571-1579 (2019).
44 <https://doi.org/10.1534/g3.119.400165>
- 45 49 Broman, K. W. *et al.* R/qt12: Software for Mapping Quantitative Trait Loci with High-
46 Dimensional Data and Multiparent Populations. *Genetics* **211**, 495-502 (2019).
47 <https://doi.org/10.1534/genetics.118.301595>
- 48 50 Gatti, D. M. *et al.* Quantitative trait locus mapping methods for diversity outbred
49 mice. *G3 (Bethesda)* **4**, 1623-1633 (2014). <https://doi.org/10.1534/g3.114.013748>
50

- 1 51 Churchill, G. A. Data Structures in QTL Viewer [https://github.com/churchill-lab/qtl-](https://github.com/churchill-lab/qtl-viewer/blob/master/docs/QTLViewerDataStructures.md)
2 [viewer/blob/master/docs/QTLViewerDataStructures.md](https://github.com/churchill-lab/qtl-viewer/blob/master/docs/QTLViewerDataStructures.md). (2017).
3 52 Vincent, M. *et al.* QTLViewer: an interactive webtool for genetic analysis in the
4 Collaborative Cross and Diversity Outbred mouse populations. *G3 (Bethesda)* **12**
5 (2022). <https://doi.org/10.1093/g3journal/jkac146>
6 53 Langfelder, P. & Horvath, S. WGCNA: an R package for weighted correlation network
7 analysis. *BMC Bioinformatics* **9**, 559 (2008). [https://doi.org/10.1186/1471-2105-9-](https://doi.org/10.1186/1471-2105-9-559)
8 [559](https://doi.org/10.1186/1471-2105-9-559)
9 54 Chesler, E. J. & Langston, M. A. in *Proceedings of the 2005 joint annual satellite*
10 *conference on Systems biology and regulatory genomics* 150–165 (Springer-Verlag,
11 San Diego, CA, USA, 2005).
12 55 Baker, E., Bubier, J. A., Reynolds, T., Langston, M. A. & Chesler, E. J. GeneWeaver:
13 data driven alignment of cross-species genomics in biology and disease. *Nucleic Acids*
14 *Res* **44**, D555-559 (2016). <https://doi.org/10.1093/nar/gkv1329>
15 56 Skelly, D. A., Raghupathy, N., Robledo, R. F., Graber, J. H. & Chesler, E. J. Reference
16 Trait Analysis Reveals Correlations Between Gene Expression and Quantitative Traits
17 in Disjoint Samples. *Genetics* **212**, 919-929 (2019).
18 <https://doi.org/10.1534/genetics.118.301865>
19

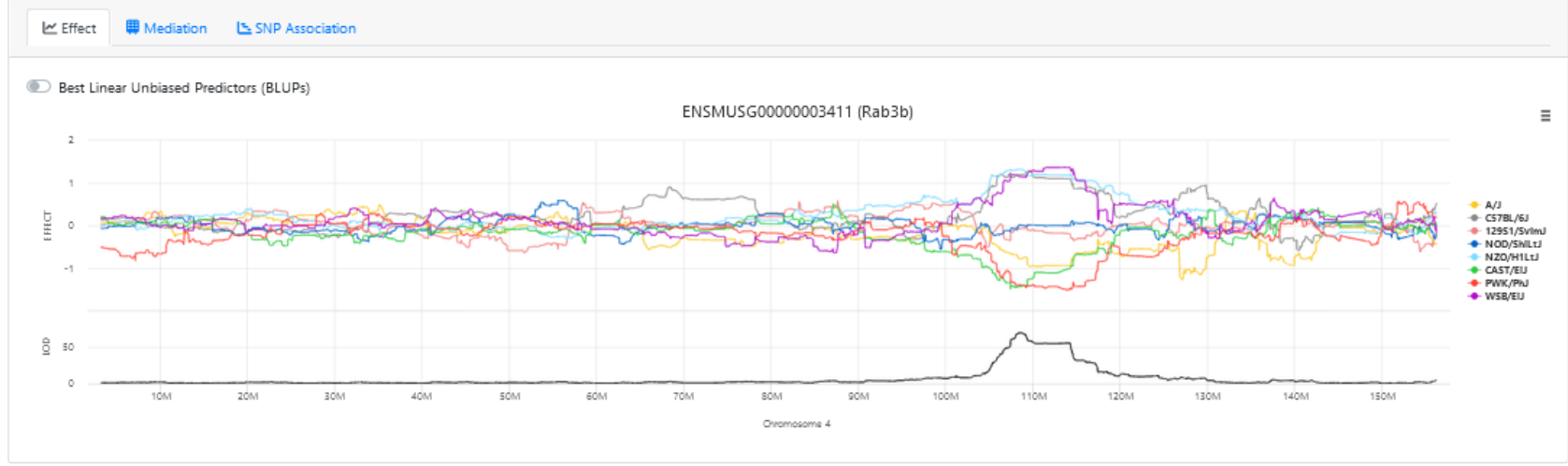
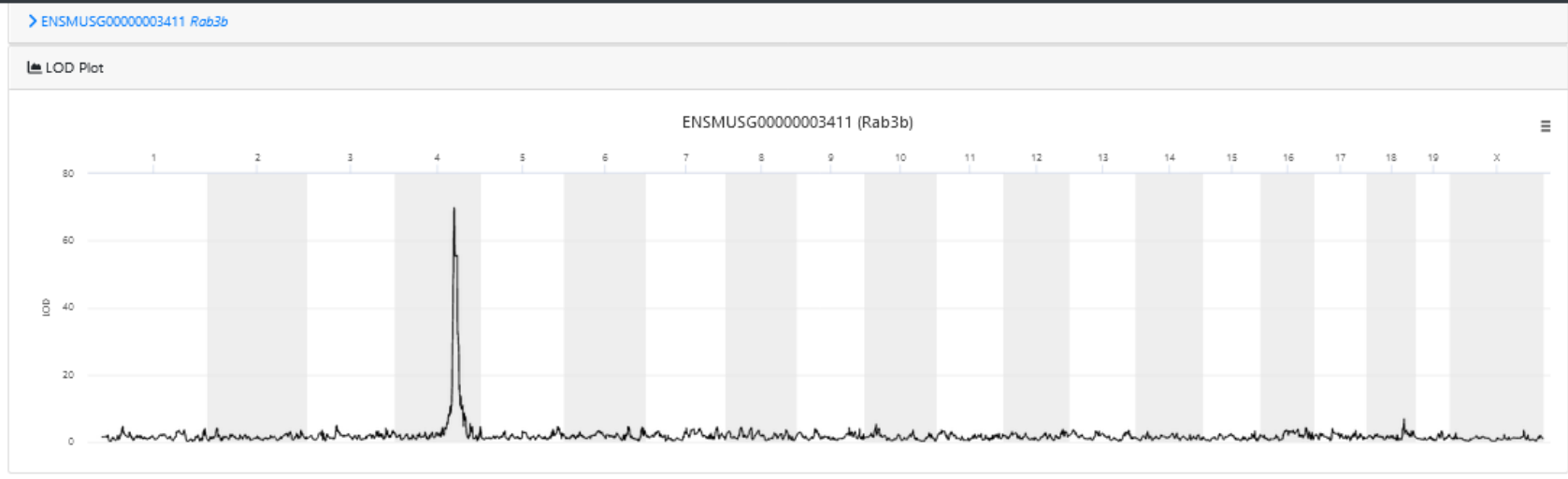
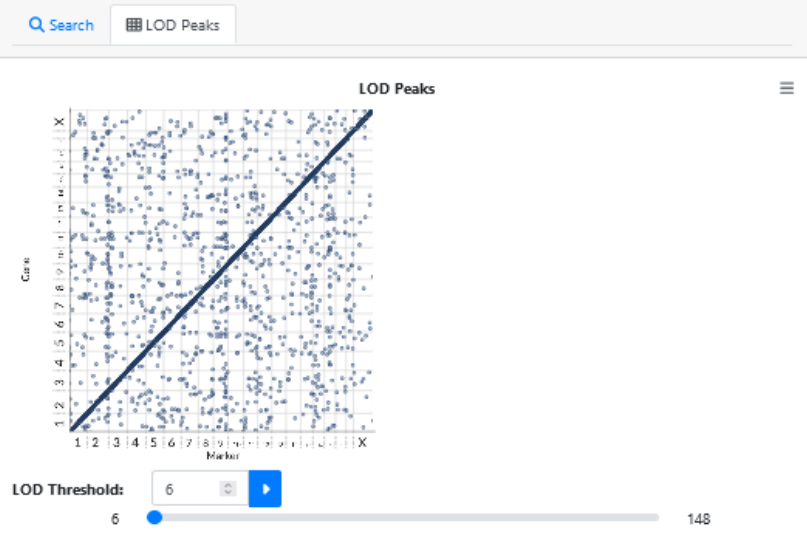


Figure 1

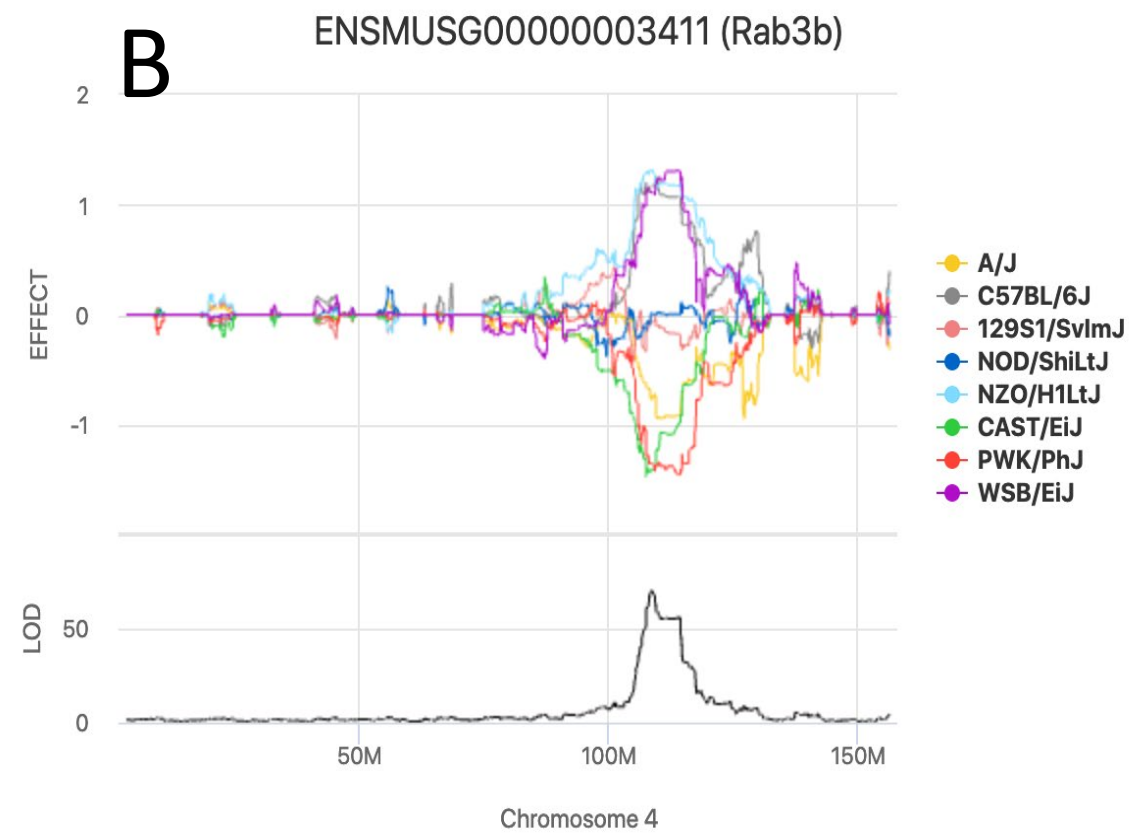
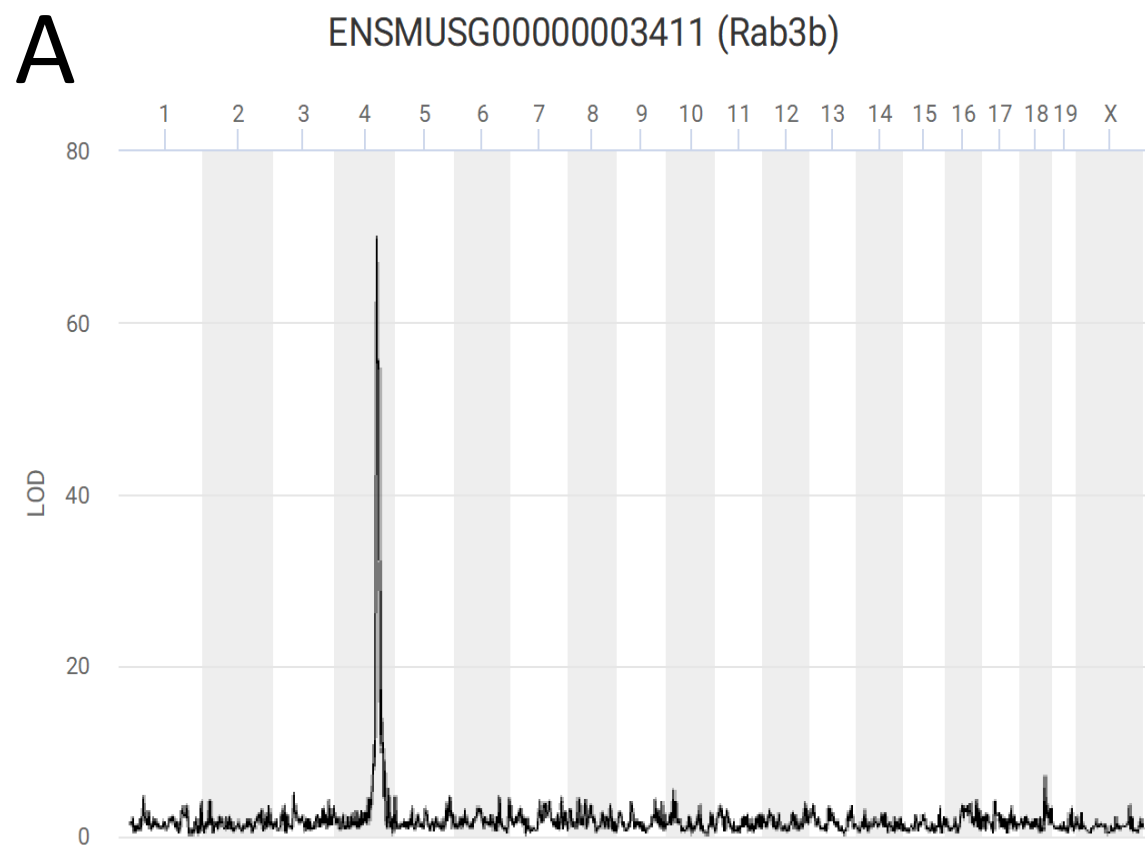


Figure 2

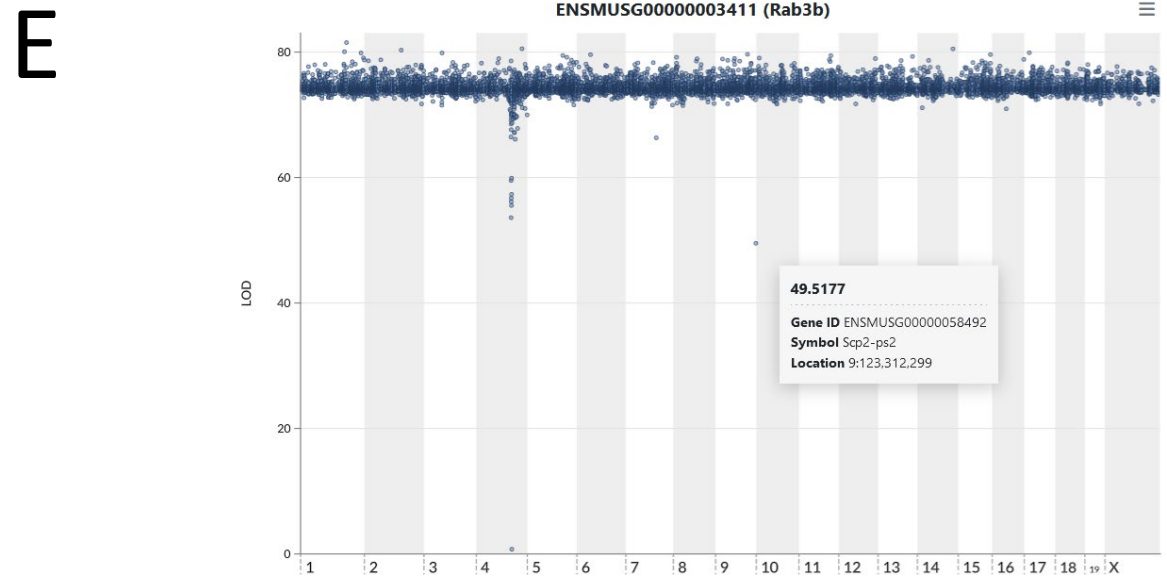
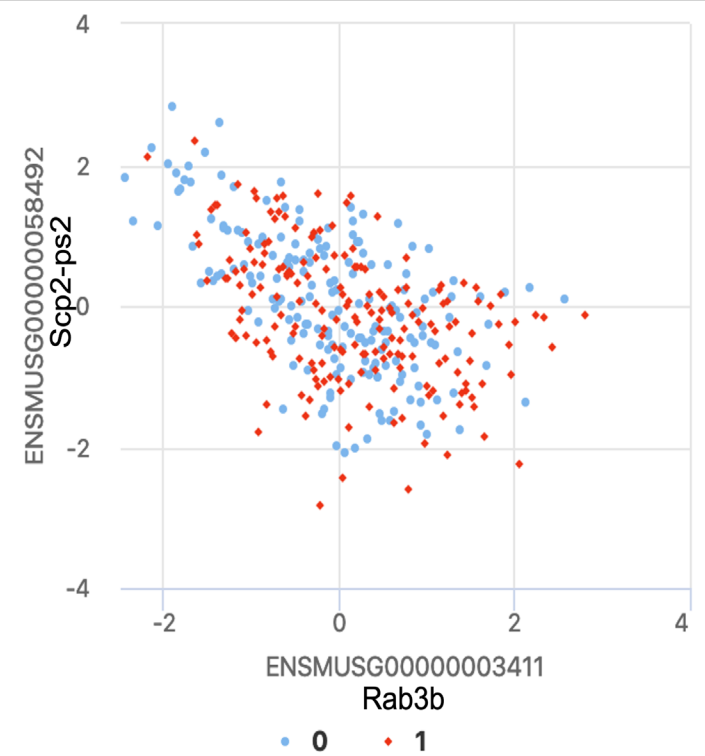
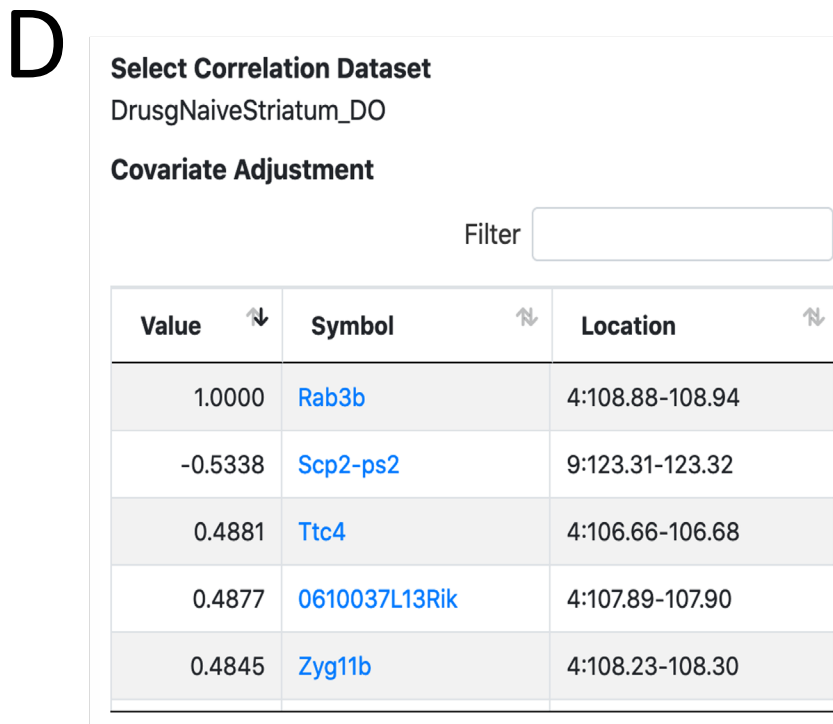
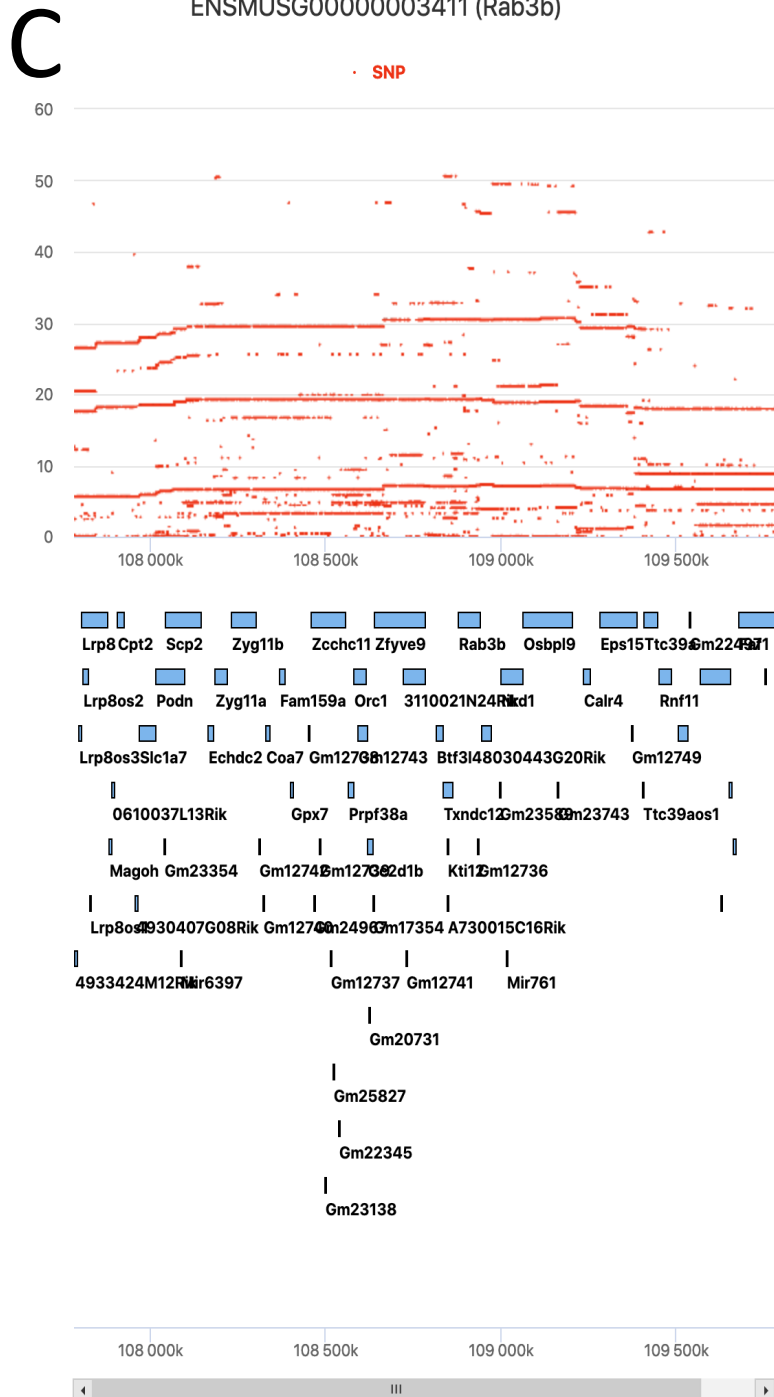


Figure 2